Inflammation, Vol. 30, Nos. 1–2, April 2007 (© 2006)
DOI: 10.1007/s10753-006-9017-8

Differential Expression, Time Course and Distribution of Four PARs in Rats with Endotoxin-induced Acute Lung Injury

Subrina Jesmin, Satoshi Gando, Sohel Zaedi, and Fumika Sakuraya

Abstract—The hypothesis that the expression of protease-activated receptors (PARs) protein is regulated at the level of transcription and that PAR isoforms, PAR-1, PAR-2, PAR-3, and PAR-4, in lung tissue show different patterns of expression in lipopolysaccharide (LPS)-induced acute lung injury (ALI) was tested. Male Wistar rats were rendered endotoxemic by intra-peritoneal injection of LPS (15 mg/kg body weight). We examined the expression of protein and mRNA and the immunohistochemical localization of PAR isoforms in lung tissues 1, 3, 6, and 10 h after LPS administration. Induction of ALI by LPS was confirmed based on histopathological changes. LPS administration induced significant increases in the expression of PAR isoforms (protein) at the level of transcription in ALI. While the time course of PAR-1 and -2 expressions were different, those of PAR-3 and -4 were almost similar. An immunohistochemical analysis showed localization of PAR isoforms in the vascular endothelium, alveolar epithelium, and alveolar macrophages. However, the cellular distribution patterns of PAR isoforms were different. We conclude that LPS induces increase in protein expression of PAR isoforms at the level of transcription in rats with ALI. The differential expression patterns (over a time course) and distribution of PAR isoforms suggests a distinct role for each isoform in the pathogenesis of LPS-induced ALI.

KEY WORDS: acute lung injury (ALI); coagulation; endotoxin; inflammation; protease-activated receptor (PAR).

INTRODUCTION

Intra-alveolar and -vascular fibrin deposition is common in acute lung injury (ALI) and acute respiratory distress syndrome (ARDS) [1,2]. The up-regulation of procoagulant pathways, impairment of physiological anticoagulant systems, and depression of the fibrinolytic pathway, collectively lead to florid alveolar fibrin deposition [3]. Fibrin deposits, in turn, enhance the inflammatory response by increasing vascular permeability, and by activating neutrophils and endothelial cells to produce proinflammatory cytokines [2, 3]. These processes are the hallmarks of ALI/ARDS and contribute to its pathogenesis. Recent evidence suggests that progressive ALI/ARDS is closely linked to the activation of inflammation and coagulation [3, 4], and that protease-activated receptors (PARs) are important candidates in this interaction [5].

To date, four distinct PAR isoforms, namely PAR-1, -2, -3, and -4 have been described. Thrombin activates PAR-1, -3, and -4, whereas, trypsin and mast cell tryptase activate PAR-2 [5–7]. Recent evidence suggests that tissue factor/factor VIIa (FVIIa) and

To whom correspondence should be addressed at Division of Acute and Critical Care Medicine, Department of Anesthesiology and Critical Care Medicine, Hokkaido University Graduate School of Medicine, N15 W7, Kita-ku, Sapporo 060, Japan. E-mail: gando@med.hokudai.ac.jp

ternary tissue factor/FVIIa/FXa complexes activate PAR-2, and PAR-1 and -2, respectively [8, 9]. Although the distribution patterns of some of the PAR isoforms have been determined in several tissues, it still remains unclear in the lungs of ALI/ARDS.

We have previously demonstrated the pulmonary expression of proinflammatory cytokine tumor necrosis factor-α (TNF) and key procoagulant molecules of tissue factor, plasminogen activator inhibitor-1 (PAI-1), and fibrin in rabbits with endotoxin-induced ALI [10]. In addition, we were able to observe increased levels of PARs protein, and to co-localize PAR-1 and procoagulant molecules in the alveolar epithelium and vascular endothelium. Collectively, these results suggest that increase in expression of PARs, together with proinflammatory cytokine and procoagulant molecules may underlie the development of ALI during endotoxemia.

The aims of the present study were to complement the data of a previous study by testing the hypothesis that: (1) the pulmonary expression of PAR isoforms (protein) is regulated at the level of transcription and that (2) the distribution pattern of each of the four PAR isoforms is distinct in the lung. To test this hypothesis, we performed experiments using a rat model of lipopolysaccharide (LPS)-induced acute lung injury.

MATERIALS AND METHODS

Animal Preparation

Male Wistar rats (200–250 g, 8 weeks old) were used in all experiments. Endotoxemia was induced by administration of bacterial LPS from *Escherichia coli* 055:B5 (15 mg/kg), dissolved in sterile saline, via I.P injection. At this dose, LPS induces lung injury, as well as the expression of inflammatory cytokines. Groups of animals (n=17) were killed using Sodium Pentobarbital (150 mg/kg bw, i.p.) at different time-points after LPS administration (1, 3, 6, and 10 h). The control group received an equal volume of sterile saline (2 ml/body), without LPS. At the indicated time, the blood samples were collected by cardiac puncture for blood gas analysis, and lung tissue specimens were harvested with care, frozen immediately in liquid nitrogen, and then stored at −80°C. For paraffin sections, lung tissue specimens were postfixed in 4% paraformaldehyde overnight and then embedded in paraffin. All the experimental procedures were approved by the Animal Care and Use Committee of Hokkaido University Graduate School of Medicine Animal Care and Use Committee.

Measurements of Hemodynamic Parameters

In order to determine the arterial blood pressure and heart rate of rats, a microtip pressure transducer catheter (SPC-320, Millar Instruments, Houston, TX, USA) was inserted into the left carotid artery of anaesthetized animals (Sodium Pentobarbital (40 mg/kg body weight, i.p.)). Then, the arterial blood pressure (BP) and heart rate (HR) were monitored using a pressure transducer (model SCK-590, Gould, Ohio, USA) and recorded (BP and HR) using a polygraph system (amplifier, AP-601G, Nihon Kohden, Tokyo, Japan; Tachometer, AT-601G, Nihon Kohden; thermal-pen recorder, WT-687G, Nihon Kohden).

Lung Wet-to-Dry Weight Ratio

Lung tissues were harvested, blotted dry and weighed in order to determine the weight of the lung in the wet state and calculate the wet-to-dry weight ratio, as follows: The lung tissues were weighed; wrapped loosely in aluminum foil; placed in a drying oven overnight; and weighed again.

Histopathology Examination

Immediately after harvest, the specimens were fixed in 4% buffered formalin solution, dehydrated, embedded in paraffin, and then sliced into 5-μm-thick sections. After deparaffinization, tissue sections were stained using standard hematoxylin and eosin (HE) staining method. Morphological injury in lung was semi-quantified by two pathologists blinded to the experimental design by analyzing, from each section, about 16 randomly selected images. The average score was then determined or calculated (n=6 rat per each group).

Immunofluorescent Labeling

For determining the cellular distribution of proteins of interest, tissue specimens were fixed in 4% buffered formalin solution, dehydrated, embedded in paraffin, and then sliced into 5-μm-thick sections. The sections were then deparaffinized and treated for 20 min with citrate buffer (10 mM citric acid, pH 6.0) in a microwave oven (750 W) before immunostaining. In some cases, frozen sections were fixed in acetone and air dried. Endogenous peroxidase activity was quenched by incubation in 3% hydrogen peroxide for 15 min. One

percent bovine albumin in Tris was used for 30 min at room temperature to block non-specific staining caused by secondary antibodies. The sections were then incubated with primary antibodies overnight at 4°C, rinsed in phosphate buffer solution and then exposed to the fluorescence secondary antibody, rhodamine-conjugated AffiniPure or fluorescein-conjugated AffiniPure anti-sheep, anti-rabbit, anti-goat or anti-mouse IgG (Jackson Immuno Research Laboratories), for 2 h according to the manufacturer's instructions. The specificity of immunoreactivity was confirmed by negative controls where nonimmune IgG was used instead of primary antibodies. The coverslips were mounted with Immunon (Thermo Shandon). Immunofluorescent images were observed using a laser scanning confocal imaging system (MRC-1024, Bio-Rad Laboratories).

Immunofluorescence staining was semi-quantitated using a scale (+ to ++++) and the average score of 20 randomly selected images was calculated. Two pathologists blinded to the experimental design evaluated each slide. The same set of experiments was repeated at least three times.

Western Blot Analysis

The immunoblotting procedure used in the present study has already been described in our previous report [11]. Briefly, ice-cold lung tissues were minced with scissors, homogenized, and centrifuged, followed by determination of protein concentration of the supernatant using the bicinchoninic acid protein assay (Pierce Biotechnology). Samples were then boiled in reducing SDS sample buffer for 5 min, loaded onto an SDS–PAGE (4–15% polyarylamide) gel under reduced conditions, subjected to electrophoresis, and electrophoretically transferred to polyvinylidine difluoride filter membrane. To reduce non-specific binding, the membrane was blocked for 2 h at room temperature with 5% non-fat milk in PBS (137 mM NaCl, 2.7 mM KCl, 8.1 mM Na_2HPO_4, 1.5 mM KH_2PO_4) containing 0.1% Tween 20, incubated overnight at 4°C with primary antibodies in PBS–Tween buffer, washed three times with PBS–Tween buffer, and then the membrane was incubated with a suitable secondary antibody coupled to horseradish peroxidase for 60 min at room temperature. The blots were washed five times in PBS–Tween buffer and subsequently visualized with an enhanced chemiluminescence detection system (Amersham), exposed to X-ray film (Fuji Photo Film). Intensity of total protein bands per lane was evaluated by densitometry. Negligible loading/transfer variation was observed between samples. In each experiment, ß-actin was used as the loading control.

Characterization of Antibodies

For immunological-based detections, the following antibodies were used: anti-human PAR-1 rabbit polyclonal antibody, anti-human PAR-2 goat polyclonal antibody, anti-mouse PAR-3 goat polyclonal antibody and anti-mouse PAR-4 goat polyclonal antibody (Santa Cruz Biotechnology); anti-rabbit fibrinogen sheep polyclonal antibody (Cedarlane Laboratories); anti-human fibrin mouse monoclonal antibody (Chemicon International), anti-rabbit inducible nitric oxide (NO) synthase (iNOS) mouse monoclonal antibody (affinity BioReagents, Golden, CO, USA), and anti-*Xenopus laevis* ß-actin mouse monoclonal antibody (Abcam). In most cases, the specificity of each antibody was initially confirmed by blocking its expression using a competing peptide against which the antibody was raised. It should also be noted that no positive immunoreactivity was observed when non-immune IgG was used instead of the primary antibodies. For PAR-1 and -2, rat liver tissue was used as positive control for both immunofluorescence staining and the immunoblot analysis, according to the manufacturer's instructions (Santa Cruz Biotechnology)[12], whereas, for PAR-3 and -4 immunoreactivities, rat liver tissue and rat uterus were used as positive controls, respectively [12]. Please note that each of the anti-PAR antibodies showed no cross-reactivity with other PAR isoforms. Anti-human fibrin mouse monoclonal antibody and anti-rabbit fibrinogen sheep polyclonal antibody recognize fibrin and fibrinogen, respectively, but can also detect each other's target peptide. The immunogen of the anti-fibrin antibody is fibrin-like ß-peptide Gly-His-Arg-Pro-Leu-Asp-Lys-Cys.

RNA Preparation and Real-Time Quantitative PCR (RT-PCR)

Total RNA samples were prepared from lung tissue specimens using the guanidinium thiocyanate-phenol-chloroform single-step extraction method with Isogen (Nippon Gene, Toyama, Japan), which is routinely used in our laboratory [11]. After isolation, the RNA was processed as follows: treated with DNase I; quantified and then reverse transcribed to cDNA by omniscript reverse transcriptase using a first-strand cDNA synthesis kit (Qiagen). The reverse transcription reaction was performed at 37°C for 60 min.

Table 1. Effects of Lipopolysaccharide (LPS) on Blood Pressures, Plasma and Pulmonary Tumor Necrosis-α (TNF) Levels and Inducible Nitric Oxide Synthase (iNOS) Induction

		LPS			
	Control	1 h	3 h	6 h	10 h
Systolic BP(mmHg)	142±4	125±8*	114±8**	108±13**	110±12**
Diastolic BP (mmHg)	94±8	82±5*	76±10*	75±12*	83±8
TNF (plasma, pg/ml)	31±20	3,606±900**	384±98**	151±91*	52±44
TNF (Lung)					
Protein (pg/ml)	3.0±0.6	40.0±13.1**	21.1±6.4**	5.1±1.0*	4.0±0.8
iNOS (Plasma, U/ml)	8.5±1.4	21.6±4.0**	15.5±3.0**	15.9±2.2**	14.7±0.7**
iNOS (Lung)					
Protein (U/mg)	1.4±0.07	1.2±0.4	1.6±0.2	3.2±0.5**	3.5±0.2**
Protein (AU)	1	1.1±0.3	1.6±0.2**	2.8±0.3**	3.3±0.4**
mRNA (%)	110±18	3,352±414**	3,064±241**	3,152±148**	804±196*

Data are mean±SD.
BP Blood pressure, *AU* arbitary unit
*$p<0.05$, **$p<0.01$ vs. control.

The expression of PAR isoform mRNAs were analyzed by real-time quantitative PCR with TaqMan probe using an ABI Prism 7700 Sequence Detector (Perkin–Elmer Applied Biosystems, Foster, CA, USA), as previously described [13]. Gene-specific primers and TaqMan probes were synthesized from Primer Express v. 1.61 software (Perkin–Elmer Applied Biosystems), according to published cDNA sequences of each gene. The sequences of the oligonucleotides were as follows:

PAR-1 forward: 5′-CCCCTTCAAGATCAGCTAC TACTTC-3′
PAR-1 reverse: 5′-GGCGAAGCGACACATTCC-3′
PAR-1 probe: 5′-CCCGAACTGCCAATCG-3′
PAR-2 forward: 5′-CCTTGAACATCACCACCT GTCA-3′
PAR-2 reverse: 5′-GGGAGAGGAAGTAACTGAACA TGTC-3′
PAR-2 probe: 5′-CCACCAGGACCTCCTC-3′
PAR-3 forward: 5′-ATCTTGTCCAACCAGGGAT CAC-3′
PAR-3 reverse: 5′-CCAAGGAGACGAAGTAGTA GAACTG-3′
PAR-3 probe: 5′-CCACGACGTCCACGACAC-3′
PAR-4 forward: 5′-GTACAGCCATGCAGTGAGACT-3′
PAR-4 reverse: 5′-GCACATTGCTAGGTGTGAA AGC-3′
PAR-4 probe: 5′-CCCTGGTCCTGTTCTC-3′
iNOS forward: 5′-GTGGGTGGCCTCGAGTTC-3′
iNOS reverse: 5′-CCAATCTCGGTGCCCATGTAC-3′
iNOS probe: 5′-CTGCCCCTTCAATGGTT-3′
ß-actin forward: 5′-GGCCGGGACCTGACA-3′
ß-actin reverse: 5′-GCTGTGGTGGTGAAGCTGTAG-3′
ß-actin probe: 5′-ACTACCTCATGAAGATCC-3′

ß-actin mRNA was used as an internal control. The PCR mixture (25 µl total volume) consisted of 450 nM of both forward and reverse primers for each gene

Table 2. Blood Gas Analysis and Lung Wet-to-Dry Weight Ratio

		LPS			
	Control	1 h	3 h	6 h	10 h
pH	7.405±0.039	7.421±0.031	7.430±0.048	7.444±0.030	7.428±0.018
$PaCO_2$ mmHg	39.4±5.7	32.3±4.1**	31.3±3.5**	30.1±5.7**	31.0±4.3**
PaO_2 mmHg	114.1±10.2	85.1±16.7**	83.3±21.7**	86.8±21.5**	89.4±17.2**
BE mM	0.2±1.0	−2.1±1.8*	−4.6±3.6**	−4.3±2.5**	−3.3±1.2**
Lactate mM	1.3±0.69	3.4±2.2**	4.9±2.9**	4.1±0.9**	4.2±1.7**
W/D ratio	4.55±0.21	5.07±0.26**	5.11±0.41**	5.36±0.12**	5.90±0.25**

Data are mean±SD.
BE base excess, *W/D* lung wet-to-dry weight ratio
*$p<0.05$, **$p<0.01$ vs. control.

(Perkin–Elmer), 200 nM of FAM-labeled primer probes (Perkin–Elmer), and TaqMan Universal PCR Master Mix (Perkin–Elmer). Each PCR amplification was performed in triplicates, using the following profile: one cycle of 95°C 10 min, and 40 cycle of 94°C for 15 s, and 60°C for 1 min. The quantitative values of target mRNAs were normalized using ß-actin mRNA expression.

Assay for Plasma and Tissue Levels of TNF and Induced Nitric Oxide Synthase (iNOS)

TNF levels in the plasma and lung tissues were detected using an enzyme-linked immunosorbent assay (ELISA) kit for screening rat TNF (Pierce Biotechnology, Rockford, IL). For iNOS, we used a Human iNOS Immunoassay kit (R and D Systems, Minneapolis, MN).

Statistical Analysis

The results were expressed as mean±SD (n=total number of animals in each group). The means were compared by a one-way factorial analysis of variance, followed by Scheffé's test for multiple comparisons. Differences were considered to be significant at a value of $p<0.05$.

RESULTS

Effects of LPS on Blood Pressures, Plasma and Pulmonary TNF Levels and iNOS Induction

As shown in Table 1, levels of both systolic and diastolic blood pressure decreased significantly after LPS administration, in comparison to control rats. The

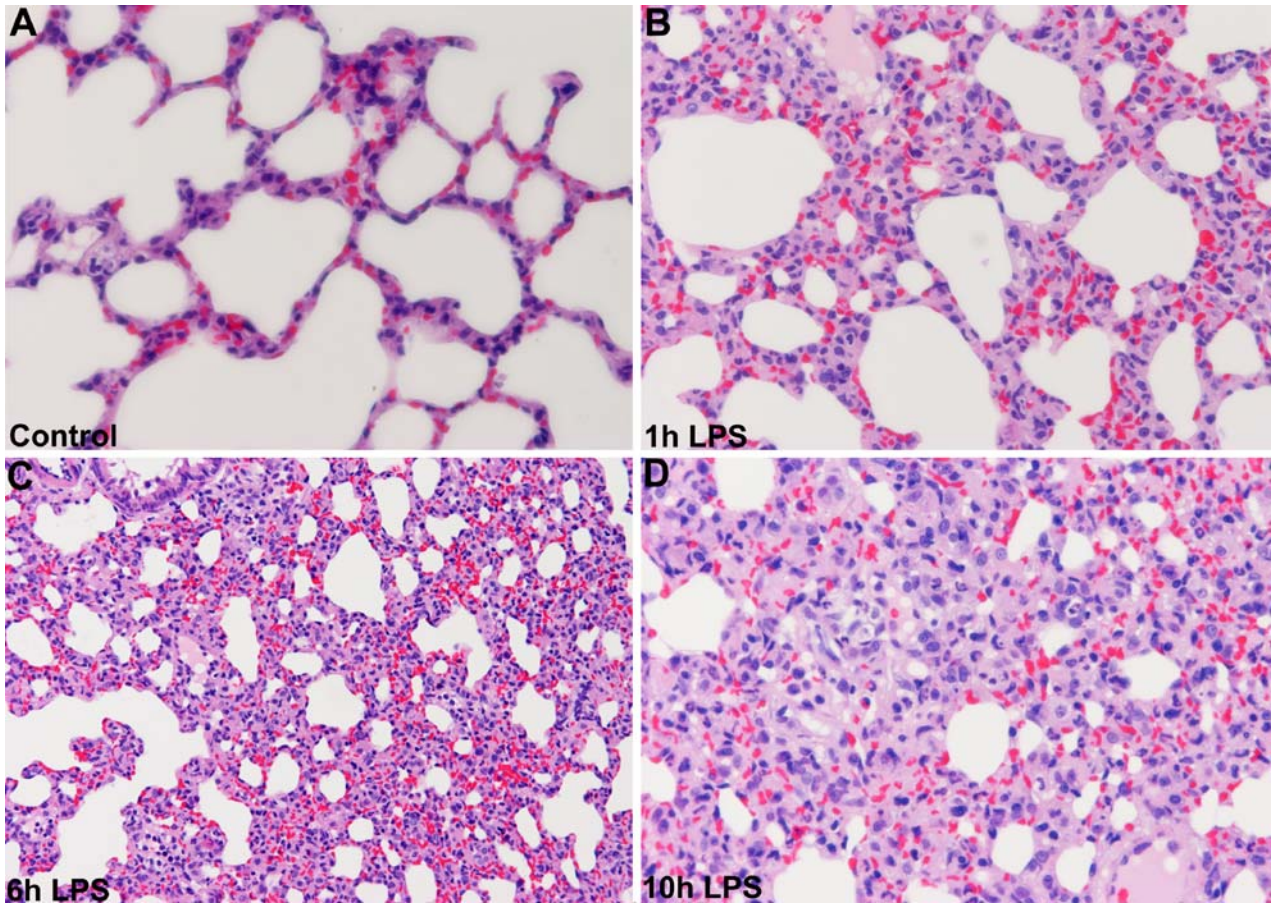

Fig. 1. Morphological findings by hematoxylin and eosin staining in lung tissue specimens from control rats and after LPS administration. Congestion, neutrophil infiltration, and thickening of alveolar septum worsened in a time-dependent manner. Magnification, ×320.

peak levels of plasma TNF and its (TNF) concentration in the lung were significantly elevated at 1 h after LPS administration. Similarly, levels of plasma iNOS and its (iNOS) protein and mRNA expression in the lung increased after LPS administration.

Assessment of ALI

Table 2 summarizes the values for blood gases and lactate concentrations in rats before and after LPS was given. Arterial PaO_2 was significantly reduced from control animals at all time points after LPS administration. As a quantitative measure of fluid clearance in lungs, wet-to-dry weight ratios were evaluated in lungs removed from rats killed at specified times after LPS administration. The effect of LPS on the ratios (wet-to-dry weight ratios) occurred in a time-dependent manner, leading to a significant (p<0.05) increase from baseline (4.5±0.2) to peak value (5.9±0.2) after LPS administration.

The lungs from control rats (untreated) showed no detectable injury, based on the histological analysis. In contrast, 1 h after LPS administration, the lungs of treated animals showed congestion (+), neutrophil infiltration (+) and thickening of alveolar septum (+). These changes were also observed at 3 and 6 h after LPS administration. At 10 h following the administra-

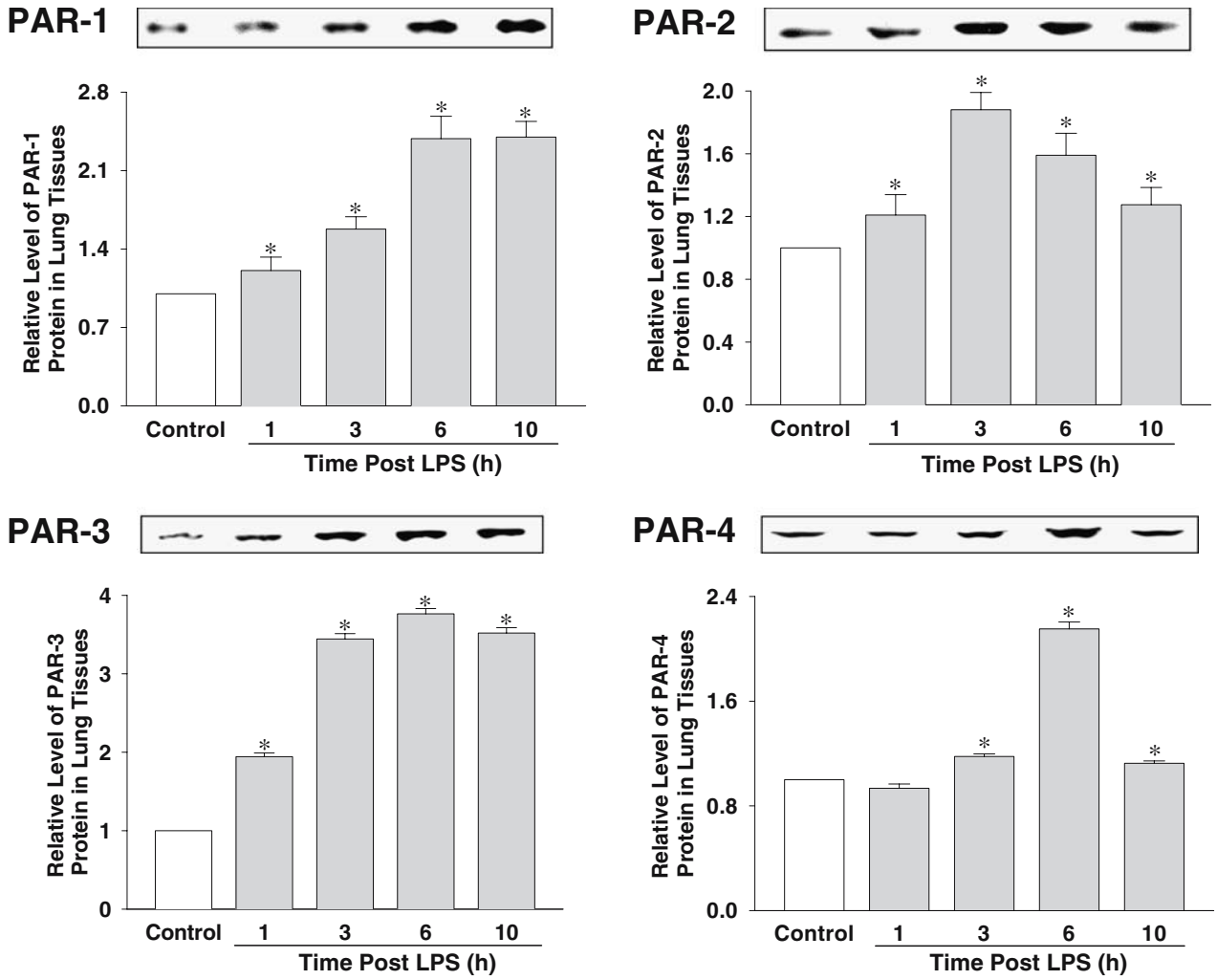

Fig. 2. An immunoblot analysis for PARs in lung tissue specimens from control and LPS-treated rats. The panel of bands shows representative blots of the type of animal and/or treatment, as described above. The intensity of the bands was plotted as histograms. In each of the experiments, the band obtained with the control was normalized as 1.0. *p<0.01 with respect to control.

tion of LPS, the features of lung injury became more evident. The lungs showed congestion (+), infiltration of inflammatory cells in the alveoli (++) and a thickening of alveolar septum (++), which together are called glanulomatous changes. These changes are shown in Fig. 1.

Effect of LPS on Pulmonary Expression of Fibrin

The relative amounts of immunodetectable fibrinogen/fibrin increased steadily following induction of sepsis with LPS. Relative levels of fibrinogen/fibrin vs. control (1.0) at 1, 3, 6, and 10 h after LPS administration were 1.6±0.015/1.5±0.04, 2.8±0.02/2.8±0.05, 3.5±0.04/7.1±0.2, and 3.6±0.03/6.3±0.2, respectively ($p<0.01$). Fibrin was poorly detectable in control lungs (data not shown). At 10 h after LPS administration, fibrin deposition was evident in the intra- and extra-vascular spaces, in the alveoli and in the bronchial epithelium (data not shown).

Western Blot and Real-Time Quantitative PCR Analyses

The PAR-1 specific antibody reacted with one band of ~62 kDa that is consistent with the predicted molecular mass of this receptor [14, 15]. Its expression increased in a time-dependent manner (Fig. 2), whereas, that of PAR-2 was observed at all time points after LPS administration, peaking (1.9-fold) 3 h after LPS administration (Fig. 2). Peak expressions of PAR-3 and -4

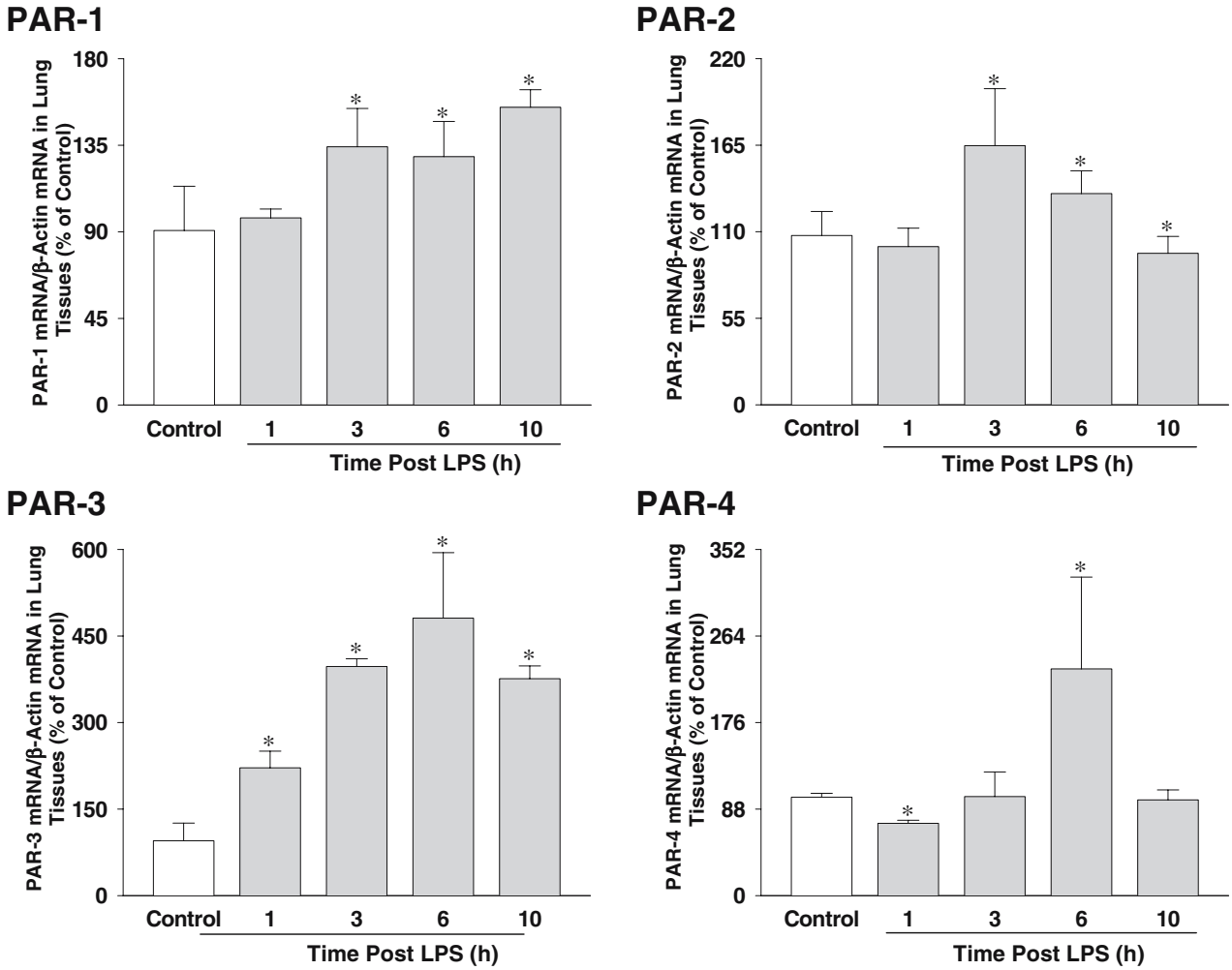

Fig. 3. A real-time-PCR analysis showing gene expressions for PARs in lung tissue specimens from the control and LPS-treated rats. The values represent the amount of mRNA relative to that in control rats (100%). *$p<0.01$ with respect to control.

proteins were seen 6 h after LPS administration (Fig. 2). PAR-2 was detected as a band of ~55 kDa, consistent with the manufacturer's information. In addition, the molecular weights of the bands believed to be those of PAR-3 and -4 were comparable to those of the Genbank sequences.

The mRNA expression of the PAR isoforms, as determined by Real-Time PCR, corresponded to levels of their respective proteins in the lung (Fig. 3).

Immunohistochemical Analyses for PARs

Immunohistochemical staining of PAR-1 (Fig. 4) in the control lung were essentially nil. However, 10 h after LPS administration, PAR-1 was predominantly expressed in the endothelium of small- to micro-sized blood vessel, and vascular smooth muscle cells of medium- to large-sized blood vessel, while only a modest expression was observed in vascular smooth muscle cells of small- micro-sized blood vessels. The endothelium of medium- to large-sized blood vessels only exhibited moderate staining of PAR-1. The alveolar epithelium and bronchial epithelium exhibited strong positive staining of PAR-1, with only modest staining observed in the alveolar macrophages.

Similar to the pattern of PAR-1 immunoreactivity, PAR-2 (Fig. 5) immunoreactivity was essentially nil in the control lungs. However, 3 h after LPS administration, it (PAR-2) was localized in the endothelium and vascular smooth muscle cells of small to micro size

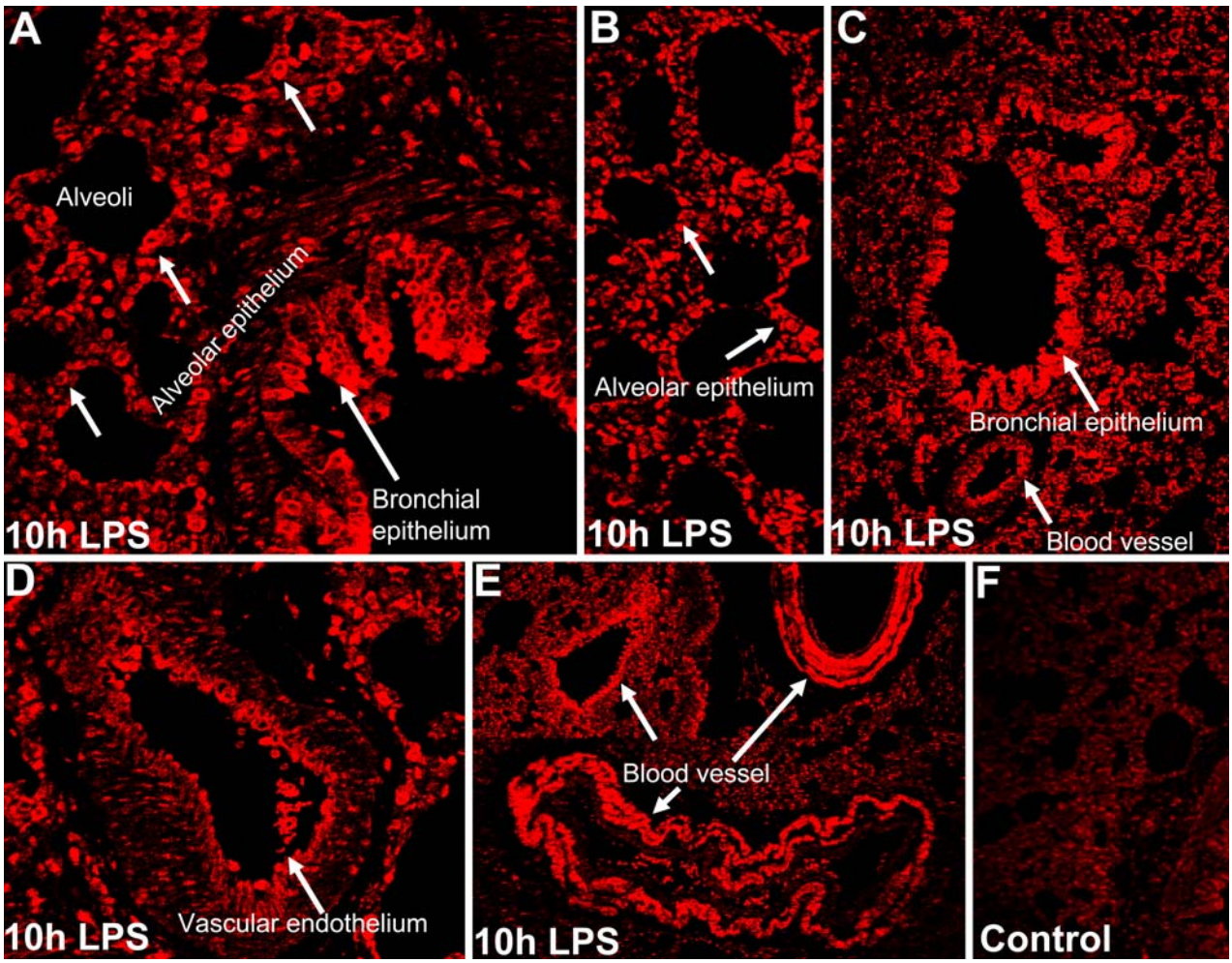

Fig. 4. Immunolocalization of PAR-1 (*red color*) in lung tissue specimens from 10 h LPS-treated rats and the control rats. PAR-1 immuonoreactivity in 10 h septic alveoli (A, B), bronchial epithelium (A, C, D), and blood vessel (C, D, E). *E*, negligible staining for PAR-1 was seen in control lung tissue specimens. Magnification, ×100.

blood vessels, at comparable intensities. In the vascular endothelium of medium- to large-sized blood vessels, PAR-2 immunoreactivity was strong, but was weakly stained in the vascular smooth muscle cells. The intensity of PAR-2 immunoreactivity in the alveolar and bronchial epithelia and alveolar macrophages were similar.

Unlike PAR-1 and -2, there was some slight immunostaining observed for PAR-3 in the control lung (Fig. 6), and by 6 h after LPS administration, it (PAR3) was intensively expressed in both the endothelium and vascular smooth muscle cells of small- to medium-sized blood vessels. In contrast, only moderate immunoreactivity was localized in the vascular smooth muscle cells of large-sized blood vessel, but nonetheless, strong staining in the endothelium. The intensity of PAR-3 immunoreactivity in the alveolar and bronchial epithelia, and alveolar macrophage, was similar to PAR-1 and -2.

Immuno-expression of PAR-4 in control lungs was similar to PAR-1 and -2 (Fig. 7), and 6 h after LPS administration, strong signals were localized in the vascular smooth muscle cells of small- to medium-sized blood vessels, and moderately expressed in the vascular endothelium. This was in contrast to the vascular endothelium of large-sized blood vessels, which exhibited strong PAR-4 immunoreactivity, with modest staining in vascular smooth muscle cells. Strong positive staining of PAR-4 is localized in alveolar epithelium, while moderate staining is observed in alveolar macrophages and the bronchial epithelium.

These results are summarized on Table 3.

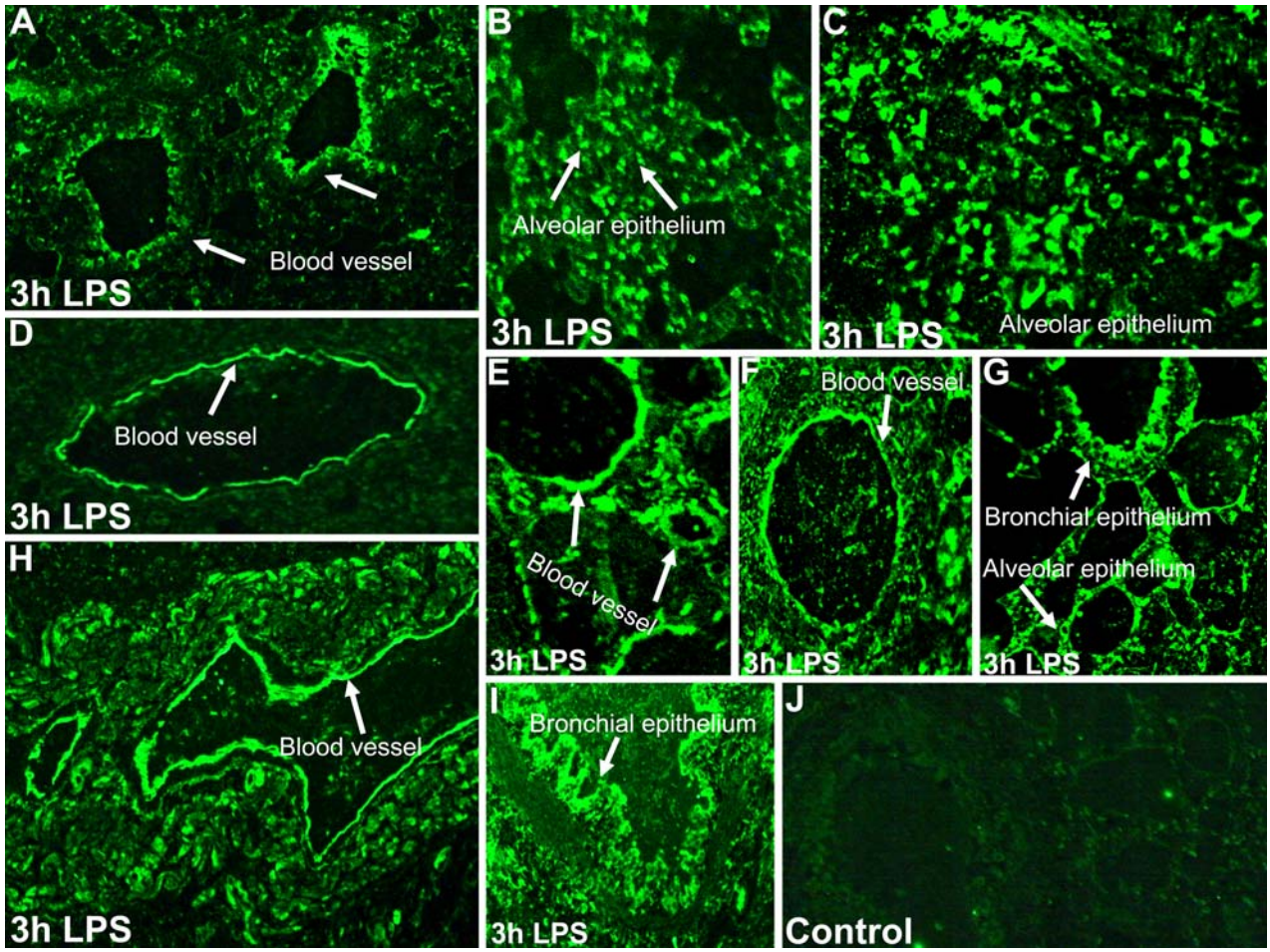

Fig. 5. Immunolocalization of PAR-2 (*green color*) in lung tissue specimens from LPS-treated and control rats. At 3 h following LPS treatment, positive staining for PAR-2 was observed in blood vessel (A, D, E, F, H), alveoli (C, B, G), and bronchial epithelium (G, I). Positive staining for PAR-2 was rare in a lung section from the control rats (J). Magnification, ×100.

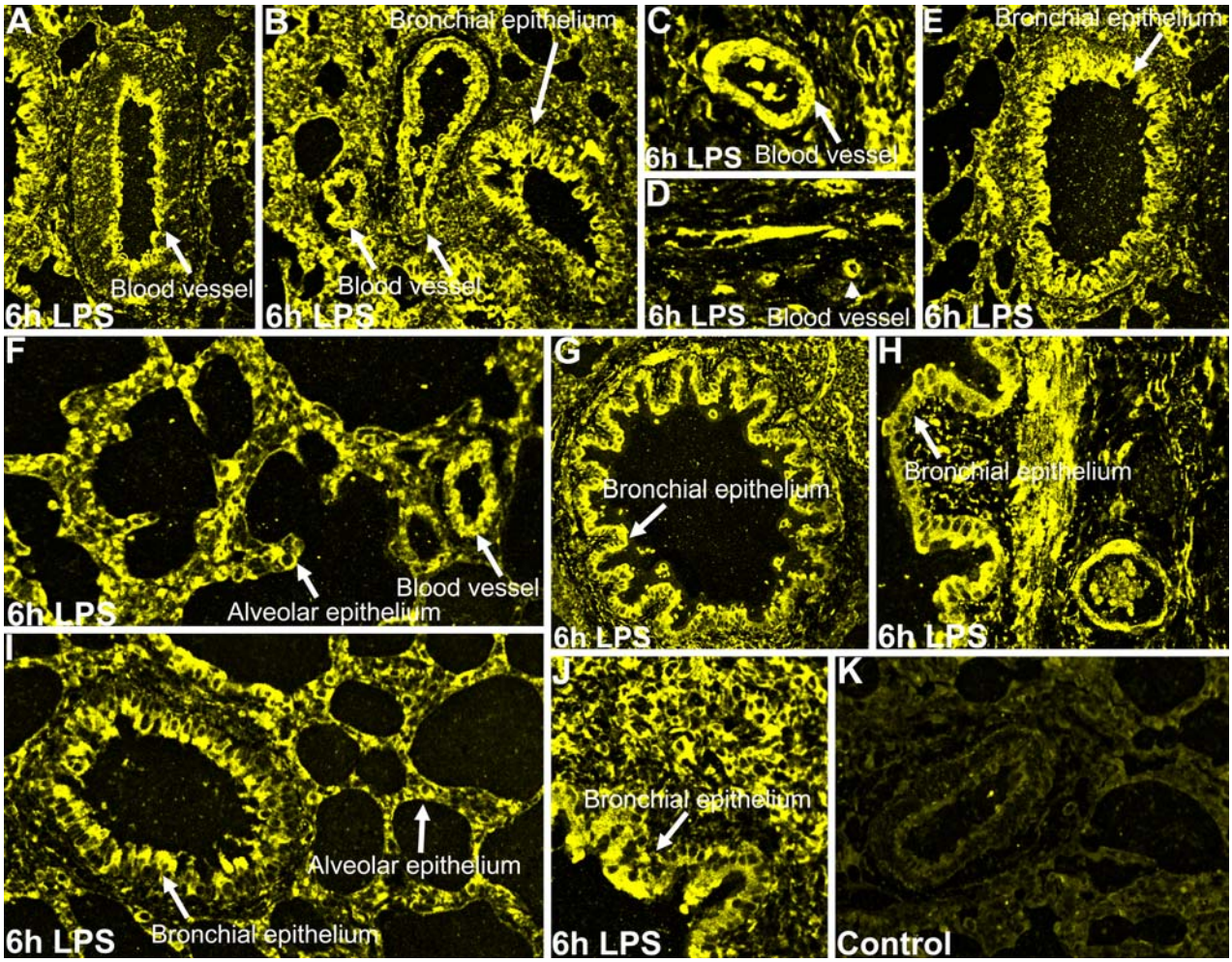

Fig. 6. Immunolocalization of PAR-3 in lung tissues from LPS-treated and the control rats. At 6 h following LPS treatment, immunoreactivities (*yellow color*) for PAR-3 were observed in blood vessel (A, B, C, D, F), alveoli (F, I) and bronchial epithelium (B, E, G, H, I, J). Control rat lung exhibited minimal staining for PAR-3 (K). Magnification, ×100.

DISCUSSION

Here, we test the hypothesis that levels of PAR isoforms in lungs are regulated at the level of transcription, but each (isoform) with a distinct pattern of tissue distribution. Following LPs administration, we observed a significant reduction in blood pressure and an increased expression of plasma iNOS, which occurred in parallel to iNOS immunoreactivity in the lung [16]. In addition, HE staining demonstrated a potent infiltration of inflammatory cells and thickening of alveolar septum called glanuloma [17]. Collectively, these findings support the notion that LPS (via i.p.) induces sepsis and the development of ALI in a rat model.

The present study observed increased expression of TNF protein in both lung tissue and plasma immediately after LPS administration. TNF is known to induce the expression of tissue factor, which leads to the activation of the extrinsic coagulation pathway, and increases in levels of FXa and thrombin, and ultimately, enhancement of coagulation [18]. TNF is also known to increase levels of PAI-1, which, in turn, inhibit fibrinolysis [18]. Following increase in TNF levels, we found a marked elevation of fibrin/fibrinogen protein levels in the lung tissues. This observation was confirmed by immunohistochemical analysis that demonstrated clear fibrin deposition in both intra-vascular and -alveolar spaces. Although, in the present study, we did not measure levels of tissue factor

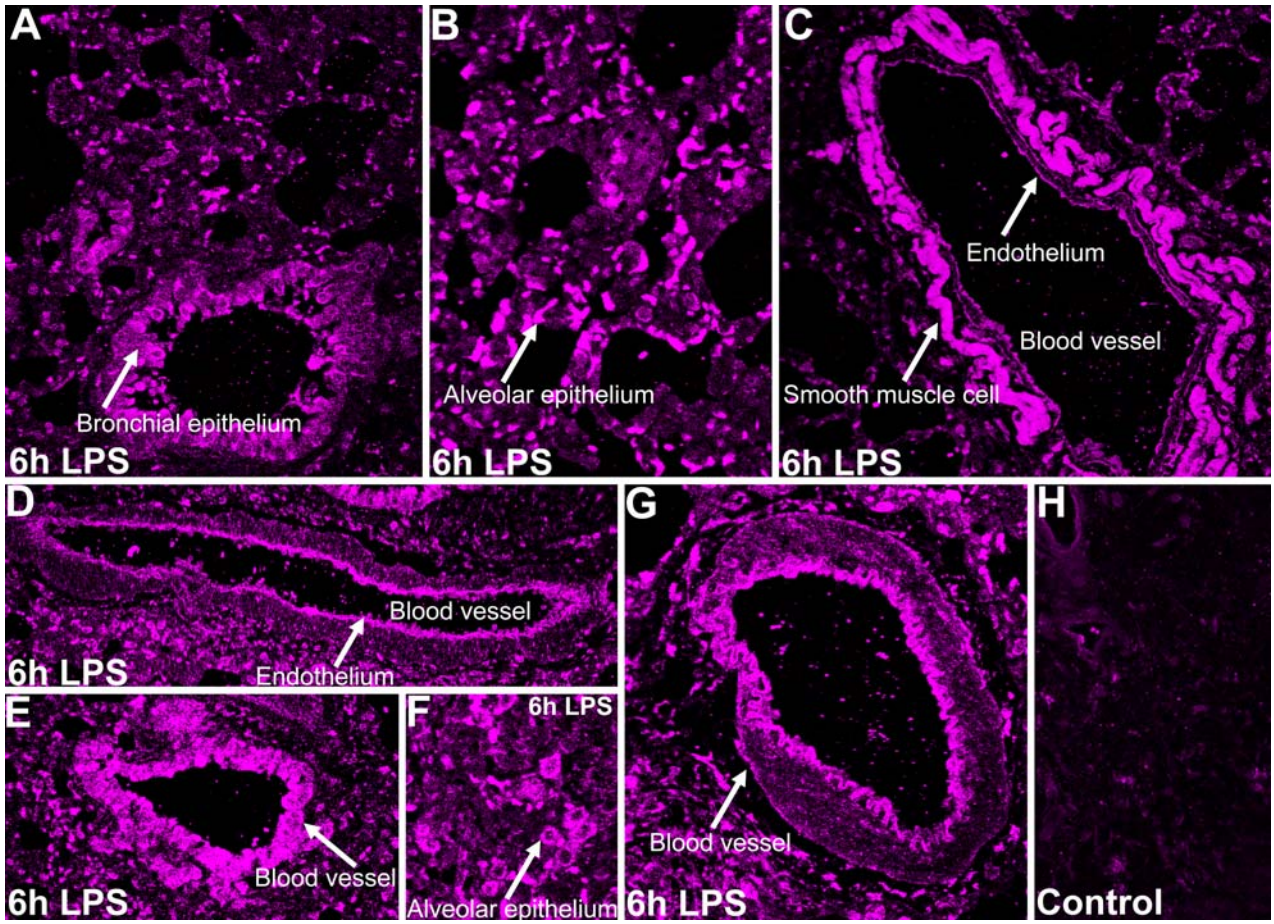

Fig. 7. Immunofluorescent findings for PAR-4 (*violet color*) in lung tissue specimens from control and LPS-treated rats. Increased positive staining for PAR-4 was found in the bronchial epithelium (A), alveoli (B, F) and blood vessel (C, D, E, G) in lung tissues from 6 h LPS-treated animals. The PAR-4 immunoreactivity was less in the lung tissue specimens from control animals (H). Magnification, ×100.

Table 3. Quantification of Immunoreactivity for Protease-Activated Receptors (PARs) in Lung Tissues at the Time of their Maximum Expression After Lipopolysaccharide (LPS) Administration

	PAR-1 (10 h)	PAR-2 (3 h)	PAR-3 (6 h)	PAR-4 (6 h)
Blood vessels (small to micro size)				
Endothelium	+++	+++	++++	++
Smooth muscle cell	+	+++	++++	++++
Blood vessels (medium to large size)				
Endothelium	+	+++	++++	++++
Smooth muscle cell	++++	+	+	+
Alveolar epithelium	+++	+++	+++	+++
Macrophage	++	++	++	++
Bronchial epithelium	++++	++++	++++	++

+ to ++++ indicate weak, moderate, strong, and prominent expressions, respectively.

or the PAI-1, in our previous investigation these molecules were highly expressed in the lung of LPS-treated rats, as revealed by Western blot and immunohistochemical analyses [10]. Collectively, these data suggest that enhanced inflammation, coagulation activation, and the inhibition of fibrinolysis lead to fibrin deposition in acutely injured lung, following LPS administration. These results are consistent with the clinical and experimental evidence for ALI and ARDS [1–4].

Here, we also found that LPS induces increases in the protein expression of PARs isoforms 1 to 4 in the lung of rats. The parallel changes observed in levels of both protein and mRNA of PAR isoforms suggests that LPS may exert its influence at the transcription level. The disparity in the timing of PARs expression between our previous and the present studies may be due to species differences [10]. Indeed, Nysted *et al*. [19] demonstrated that stimulation with the cytokines TNF and interleukin-1 (IL-1), as well as bacterial LPS resulted in a five to ten fold elevation of PAR-2 gene expression in a dose-dependent manner using HUVEC. In addition, the exogenous treatment of human skeletal muscle cell and monocyte with proinflammatory cytokines increased expression of PAR-1 and -2 [20, 21]. Lan *et al*. [22] demonstrated that inflammatory stimuli induced by influenza A virus expressed PAR-1, -2, -3, and -4 mRNA in the lung of intact mice. It is interesting to note that the occurrence of peak levels for plasma and lung TNF (1 h after LPS administration), coincided with the point at which significant elevations of PARs-1,-2, and-3 were observed, compared to control. These results suggest that TNF, together with, or as well as, LPS rapidly induce expression of PARs gene expression through transcription factors in the injured rat lungs.

Nuclear factor-kappaB (NF-kB) is a transcriptional factor that plays a critical role in sepsis by regulating gene expression of many inflammatory cellular mediators and receptors involved in immune recognition [23]. The NF-kB activators include an extensive list of gram-positive and -negative bacteriae and their products such as LPS; viruses and their components; protozoan parasites; cytokines (e.g., TNF, IL-1); free radical; and oxidants. Although determination of factors likely to regulate the transcription of PARs is important, it goes beyond the aims of the present study. We believe that NF-kB may be one of the most important transcriptional factors regulating PARs expression in LPS-induced ALI and, as such, plan study it in our future projects.

Although little is known about the cellular distribution of PAR-3 and -4 in lung tissue, PARs-1 and -2 have been demonstrated in the airway epithelial and smooth muscle cells within the respiratory tract, as well as endothelial and vascular smooth muscle cells [24]. PAR-1 and -2 are also present in the terminal bronchial epithelium and Type II epithelial cells of the peripheral lung, and lung macrophages, mast cells, granulocytes, and lymphocytes [24]. While our previous study demonstrated the immunolocalization of PAR-1 in these cells and tissues in LPS-treated rabbits, the present study showed strong immunoreactivities for all isoforms of PARs in the endothelium, alveolar epithelium, and lung macrophages using a rat model of ALI [10]. In addition to increased immunoreactivities of tissue factor and PAI-1 in the endothelium and alveolar epithelium, as reported in the previous study, we also confirmed here a strong fibrin deposition in the alveolar epithelium, and intra-alveolar and -vascular spaces. Both the endothelium and alveolar epithelium are known to play important roles in the pathogenesis of ALI. The co-localization of the key procoagulant molecules and the four isoforms of PAR in these tissues imply that these molecules may also play a pivotal role in inducing permeability in endothelial and epithelial cells, as observed in LPS-induced ALI.

In contrast to the distinct patterns in onset and course of expression, and localizations of PAR-1 and -2, PAR-3 and -4 had almost a similar pattern. It has been suggested that, in certain instances, binding of protease to one receptor can facilitate cleavage of another receptor. This appears to be the case for PAR-3 and -4 on mouse platelets [25]. Other studies suggest that PAR-3 facilitates activation of PAR-4 in the presence of low thrombin concentration [25, 26]. Some data indicate that PAR-3 is a cofactor for PAR-4 in mouse platelets: the hirudin-like site of PAR-3 binds and concentrates thrombin at the cell surface, and, thereby, promote cleavage of thrombin to PAR-4 [26]. While the pathological significance of these phenomena has not been elucidated, the co-localization and co-expression of PAR3 and -4, as observed in the present study, may indicate a similar cofactor relationship.

A recent study provides strong evidence that neutrophil elastase-mediated apoptosis plays a pivotal role in the pathogenesis of ALI, through the PAR-1-dependent pathway [27]. Vogel *et al*. [28] demonstrated abrogation of thrombin-induced increase in pulmonary microvascular permeability in PAR-1 knockout mice. Furthermore, the absence of PAR-1 signaling appears to attenuate bleomycin-induced lung inflammation and fibrosis [29]. Indeed, using PAR-2 knockout mouse, Su *et al*. [30] demonstrated that PAR-2 activation induces lung inflammation and pulmonary edema. In

addition to these studies, we found expression of PAR-1 and -2 and their localization in endothelium, alveolar epithelium and macrophages in the lung. Taken together, these data suggest that PAR-1 and -2 may play a critical role in the pathogenesis of ALI. However, the physiological and or pathological significance of PAR-3 and -4 expressions in the injured lung is currently unclear.

The limitations of the present study include: (1) a narrow window of time after administration of LPS was investigated to study the pulmonary expression of PARs; (2) the single moderate dose of LPS (and not higher dose), although able to induce endotoxemia in rat, could not induce severe endotoxemia. Thus, the current investigation could not provide insights on PARs expression patterns associated with severe endotoxemia. For this reason, future studies should investigate a possible correlation between the degree of severity of induced endotoxemia and the pattern of PARs expression. In addition, a more extended and prolonged time course study should be undertaken that will enable examination of the pulmonary PARs expression possible.

In summary, we demonstrate expression of PAR-1, -2, -3, and -4 proteins, which occurred at the level of mRNAs for up to 10 h after LPS administration in a rat model of ALI. The timing in expression, i.e., in onset and over the course of time, for the four isoforms of PARs were distinct. They were also localized in diverse cells, including vascular endothelium, alveolar epithelium, and alveolar macrophages, a similar localization pattern as tissue factor and PAI-1, observed in our previous study. In addition, we also found TNF expression, as well as intra-alveolar and -vascular fibrin deposition in the lung. Collectively, these results suggest that each PAR isoform plays a distinct important role in the pathogenesis of LPS-induced ALI.

ACKNOWLEDGEMENTS

This work was supported by a Grant-in-Aid for Scientific Research from the Ministry of Education, Science, Sports and Culture of Japan (2005-17390479). The authors thank Dr. Chishimba N Mowa for his professional proofreading and helpful suggestions.

REFERENCES

1. Idell, S. 2003. Coagulation, fibrinolysis, and fibrin deposition in acute lung injury. *Crit. Care. Med.* **31**(suppl):S213–S220.
2. Abraham, E. 2000. Coagulation abnormalities in acute lung injury and sepsis. *Am. J. Respir. Cell. Mol. Biol.* **22**:401–404.
3. Levi, M., M. J. Schultz, A. W. Rijneveld, and T. van del Poll. 2003. Bronchoalveolar coagulation and fibrinolysis in endotoxemia and pneumonia. *Crit. Care. Med.* **31**(suppl):S238–S242.
4. Welty-Wolf, K. E., M. S. Carraway, T. Ortel, and C. A. Piantadosi. 2002. Coagulation and inflammation in acute lung injury. *Thromb. Haemost.* **88**:17–25.
5. Coughlin, S. R. 2000. Thrombin signaling and protease-activated receptors. *Nature* **407**:258–264.
6. Dély, O., C. U. Corvera, M. Steinhoff, and N. E. Bunnett. 1998. Proteinase-activated receptors: novel mechanisms of signaling by serine proteases. *Am. J. Physiol., Cell. Physiol.* **74**(43):C1429–C1452.
7. Macfarlane, S. R., M. J. Seatter, T. Kanke, G. D. Hunter, and R. Plevin. 2001. Proteinase-activated receptors. *Pharmacol. Rev.* **53**:245–282.
8. Leadley, R. L. Jr., L. Chi, and A. R. Porcari. 2001. Non-hemostatic activity of coagulation factor Xa: potent implications for various diseases. *Curr. Opin. Pharmacol.* **1**:169–175.
9. Camerer, E., W. Huang, and S. R. Coughlin. 2000. Tissue factor- and factor X-dependent activation of protease-activated receptor 2 by factor VIIa. *Proc. Natl. Acad. Sci. U. S. A.* **97**:5255–5260.
10. Jesmin, S., S. Gando, N. Matsuda, I. Sakuma, S. Kobayashi, F. Sakuraya, and Y. Hattori. 2004. Temporal changes in pulmonary expression of key procoagulant molecules in rabbits with endotoxin-induced acute lung injury: elevated expression levels of protease-activated receptors. *Thromb. Haemost.* **92**:966–979.
11. Jesmin, S., I. Sakuma, A. Salah-Eldin, K. Nonomura, Y. Hattori, and A. Kitabatake. 2003. Diminished penile expression of vascular endothelial growth factor and its receptors at the insulin-resistant stage of a type II diabetic rat model: a possible cause for erectile dysfunction in diabetes. *J. Mol. Endocrinol.* **31**:401–418.
12. Chien, E. K., L. Sweet, M. Phillippe, S. Marietti, T. T. Kim, D. A. Wolff, L. Thomas, and E. Bieber. 2003. Protease-activated receptor isoform expression in pregnant and nonpregnant rat myometrial tissue. *J. Soc. Gynecol. Investig.* **10**:460–468.
13. Maeda, S., T. Miyauchi, and M. Iemitsu. 2002. Effects of exercise training on expression of endothelin-1 mRNA in the aorta of aged rats. *Clin. Sci. (Lond.)* **103**(Suppl 48):118S–123S.
14. Copple, B. L., F. Moulin, U. M. Hanumegowda, P. E. Ganey, and R. A. Roth. 2003. Thrombin and protease-activated receptor-1 agonists promote lipopolysaccharide-induced hepatocellular injury in perfused liver. *J. Pharmacol. Exp. Ther.* **305**:417–425.
15. Launza, M. A., N. Garcia, C. M. González, M. M. Santaé, P. G. Nelson, and J. Tomas. 2003. Role of expression of thrombin receptor PAR-1 in muscle cells and neuromuscular junctions during the synapse elimination period in the neonatal rat. *J. Neurosci. Res.* **73**:10–21.
16. Buttery, L. D., T. J. Evans, D. R. Springall, A. Carpenter, J. Chohen, and J. M. Polak. 1994. Immunochemical localization of inducible nitric oxide synthase in endotoxin-treated rats. *Lab. Invest.* **71**:755–764.
17. Wright, J. L. 1999. The pathology of ARDS. In: J. A. Russel and K. R. Walley (eds). *Acute Respiratory Distress Syndrome. A comprehensive clinical approach.* Cambridge, UK, Cambridge University Press, pp 48–62.
18. Levi, M., H. ten Cate, T. van der Poll, and S. J. H. van Deventer. 1993. Pathogenesis of disseminated intravascular coagulation in sepsis. *JAMA* **270**:975–979.
19. Nystedts, S., V. Ramakrishnan, and J, Sundelin. 1996. The proteinase-activated receptor 2 is induced by inflammatory mediators in human endothelial cells. Comparison with the thrombin receptor. *J. Biol. Chem.* **27**:14910–14915.
20. Mbebi, C., T. Rohn, M. A. Doynnette, F. Chevessier, M. Jandrot-

Perrus, D. Hantal, and M. Verdiere-Sahuque. 2001. Thrombin receptor induction by injury-related factors in human skeletal muscle cells. *Exp. Cell. Res.* **263**:77–87.
21. Naldini, A., L. Sower, V. Bocci, B. Meyers, and D. H. Carney. 1998. Thrombin receptor expression and responsiveness of human monocytic cells to thrombin is linked to interferon-induced cellular differentiation. *J. Cell. Physiol.* **177**:76–84.
22. Lan, R. S., G. A. Stewart, R. G. Goldie, and P. J. Henry. 2003. Altered expression and *in vivo* lung function of protease-activated receptors during influenza A virus infection in mice. *Am. J. Physiol., Lung Cell. Mol. Phsysiol.* **286**:L388–L398.
23. Zingarelli, B. 2005. Nuclear factor-kB. *Crit. Care. Med.* **33**(Suppl): S414–S416.
24. Lan, R. S., G. A. Stewart, and P. J. Henry. 2002. Role of protease-activated receptors in airway function: a target for therapeutic intervention? *Pharmacol. Ther.* **95**:239–257.
25. Nakanishi-Matsui, M., Y. W. Zheng, D. J. Sulcinar, E. J. Weiss, M. J. Ludeman, and S. R. Coughlin. 2000. PAR3 is a cofactor for PAR4 activation by thrombin. *Nature* **404**:609–613.
26. Coughlin, S. R. 2005. Protease-activated receptors in hemostasis, thrombosis and vascular biology. *J. Thromb. Haemost.* **3**:1800–1814.
27. Suzuki, T., T. J. Moraes, E. Vachon, H. H. Ginzberg, T. T. Huang, M. A. Matthay, M. D. Hollenberg, J. Marshall, C. A. G. McCullock, M. T. H. Abreu, C. W. Chow, and G. P. Downey. 2005. Protease-activated receptor-1 mediates elastase-induced apoptosis of human lung epithelial cells. *Am. J. Cell. Mol. Biol.* **33**:231–247.
28. Vogel, S. M., X. Gao, D. Mehta, R. D. Ye, T. A. John, P. Andrade-Gordon, C. Tiruppathi, and A. B. Malik. 2000. Abrogation of thrombin-induced increase in pulmonary microvascular permeability in PAR-1 knockout mice. *Physiol. Genomics.* **4**:137–145.
29. Howell, D. C. J., R. H. Johns, J. A. Lasky, B. Shan, C. J. Scotton, G. J. Laurent, and R. C. Chambers. 2005. Absence of protease-activated receptor-1 signaling affords protection from bleomycin-induced lung inflammation and fibrosis. *Am. J. Pathol.* **166**:1353–1365.
30. Su, X., J. R. Hamilton, S. R. Coughlin, and M. A. Matthay. 2005. Protease-activated receptor-2 activation induces acute lung inflammation by neuropeptide-dependent mechanisms. *J. Immunol.* **175**:2598–25605.